JACS
JOURNAL OF THE AMERICAN CHEMICAL SOCIETY
Communication
pubs.acs.org/JACS

Diastereoselective Imine-Bond Formation through Complementary Double-Helix Formation

Hidekazu Yamada, Yoshio Furusho, and Eiji Yashima*

Department of Molecular Design and Engineering, Graduate School of Engineering, Nagoya University, Chikusa-ku, Nagoya 464-8603, Japan

Supporting Information

ABSTRACT: Optically active amidine dimer strands having a variety of chiral and achiral linkers with different stereostructures are synthesized and used as templates for diastereoselective imine-bond formations between two achiral carboxylic acid monomers bearing a terminal aldehyde group and racemic 1,2-cyclohexanediamine, resulting in a preferred-handed double helix stabilized by complementary salt bridges. The diastereoselectivity of the racemic amine is significantly affected by the chirality of the amidine residues along with the rigidity and/or chirality of the linkers in the templates. NMR and kinetic studies reveal that the present imine-bond formation involves a two-step reversible reaction. The second step involves formation of a preferred-handed complementary double helix assisted by the chiral amidine templates and determines the overall reaction rate and diastereoselectivity of the amine.

Template-directed polymerization, or template synthesis,[1,2] is ubiquitous in nature, as exemplified by the nucleic acid-templated polymerization that is capable of replication, transcription, and translation of the genetic information of the nucleic acids through non-covalent bonding interactions, providing DNA, RNA, and proteins with perfectly controlled sequences and chain lengths as well as chirality. Non-enzymatic template-directed syntheses have been used to construct oligonucleotide analogues,[3−6] peptides,[7] and small abiotic organic molecules[8] and polymers.[1a,2a,c,f,9] The key factor necessary for template-directed polymerization and synthesis is a complementary interaction between the template and the monomers; nucleotides and nucleobases and their related molecules or polymers have frequently been employed as templates. The helically twisted structure of the DNA templates also promoted a stereoselective chemical reaction when the reactive groups were positioned at each strand in such a way that nucleophilic substitution took place,[5] but template-directed asymmetric or diastereoselective reactions are quite limited except for DNA.[10]

We previously designed and synthesized artificial double-stranded (ds) helices[11] consisting of complementary molecular strands intertwined through amidinium-carboxylate salt bridges.[12] The well-defined geometry and high association constants of the salt bridges prompted us to prepare novel complementary double helices bearing various types of linkers and possessing a helix-sense bias induced by the chiral amidine groups. We also reported template synthesis of a complementary carboxylic acid dimer through an imine-bond formation along the template amidine dimer assisted by salt bridges, showing remarkable acceleration of the imine-bond formation assisted by the template during double-helix formation.[13]

Chart 1. Structures of Chiral Amidine Templates

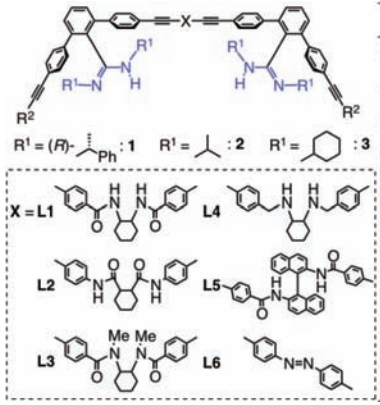

template	R^2	X
(*R*,*R*,*R*,*R*,*R*,*R*)-**1a**	TMS	(*R*,*R*)-**L1**
(*R*,*R*,*S*,*S*,*R*,*R*)-**1b**	TMS	(*S*,*S*)-**L1**
(*R*,*R*,*R*,*R*,*R*,*R*)-**1c**	TMS	(*R*,*R*)-**L2**
(*R*,*R*,*S*,*S*,*R*,*R*)-**1d**	TMS	(*S*,*S*)-**L2**
(*R*,*R*,*R*,*R*,*R*,*R*)-**1e**	TMS	(*R*,*R*)-**L3**
(*R*,*R*,*R*,*R*,*R*,*R*)-**1f**	TMS	(*R*,*R*)-**L4**
(*R*,*R*,*R*,*R*,*R*)-**1g**	TMS	(*R*)-**L5**
(*R*,*R*,*R*,*R*)-**1h**	TMS	**L6**
(*R*,*R*)-**2a**	TMS	(*R*,*R*)-**L1**
(*R*,*R*)-**2b**	H	(*R*,*R*)-**L4**
(*R*,*R*)-**3a**	TMS	(*R*,*R*)-**L1**

We have now designed and synthesized optically active amidine dimers consisting of (*R*)-1-phenylethyl amidine (**1**) and achiral isopropyl (**2**) and cyclohexyl amidines (**3**) with an *m*-terphenyl backbone linked through chiral (**L1**−**L5**) and achiral (**L6**) linkers (Chart 1). Amidine dimers **1**−**3** were used as optically active templates on which imine-bond formation takes place when a terminal aldehyde group on the complementary achiral carboxylic acid monomer **A** reacts with the racemic *trans*-1,2-cyclohexanediamine **B** along the templates, producing carboxylic acid dimer $\mathbf{A}_2\mathbf{B}$ complexed with the template through salt bridges (Scheme 1). We anticipated that the imine-bond formation between **A** and **B** could proceed diastereoselectively assisted by the chiral templates, forming ds helical dimers with controlled helical sense.

Imine-bond formation was used in this study because it requires no catalyst and is well established in modern organic chemistry[14] and DNA-templated polymerization of nucleobase analogues.[4,6] Imine-bond formation between **A** and (*S*,*S*)-**B** was first conducted using the chiral amidine dimer **1a** as a template linked by (*R*,*R*)-*trans*-cyclohexanediamine through an amide

Received: February 13, 2012
Published: April 16, 2012

   dx.doi.org/10.1021/ja301430h | *J. Am. Chem. Soc.* 2012, 134, 7250−7253

Scheme 1. Diastereoselective Imine-Bond-Formation through Complementary Double-Helix Formation

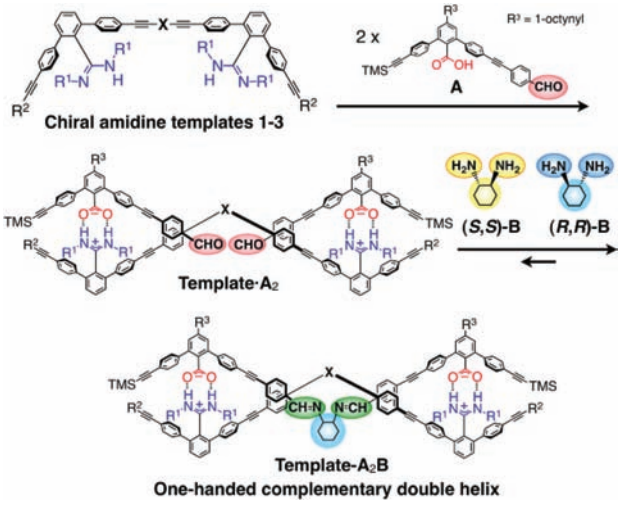

bond (**L1**) in $CDCl_3$ at 25°C; the reaction's progress was monitored by ^{1}H NMR spectroscopy (Figures 1a and S1a). ^{1}H NMR spectra of the mixtures of 1.0 mM **A** and 0.5 mM (*S*,*S*)-**B** in the presence of 0.5 mM **1a** showed resonances of NH protons at the low magnetic field of 13.25 ppm, indicating salt bridge formation (Figure S1a). The peak intensity of the aldehyde proton (H_a) of **A** decreased with time, while two new kinds of imino proton peaks appeared (H_b, H_c), suggesting imine-bond formation. The peak intensity of H_c gradually increased with time, whereas that of H_b decreased and almost disappeared. Taking into account these spectral changes along with the fact that the imine-bond formations between **A** and **B** are likely two-step reversible reactions (Figure 1), peaks H_b and H_c were reasonably assigned to the protons corresponding to monoimine intermediate **AB** and carboxylic acid dimer $\mathbf{A_2B}$, respectively, indicating duplex $\mathbf{1a{\cdot}A_2B}$ formation, which was also supported by negative-mode electrospray ionization mass spectrometry, which exhibited a molecular ionic peak at m/z = 2808.0 corresponding to $[\mathbf{1a{\cdot}A_2B}-H]^-$ (Figure S2). The reaction reached equilibrium within 9 h, and no detectable ^{1}H NMR change was observed after 1 day. Reaction between **A** and (*R*,*R*)-**B** in the presence of the identical **1a** template (Figures 1b and S1b) proceeded faster than that with (*S*,*S*)-**B**, reaching equilibrium within 3 h. In addition, the peak intensity of the imino proton (H_b) derived from the monoimine intermediate **AB** was very weak even during the initial stage, indicating that the second imine-bond formation proceeded immediately after the first.[15]

Time-dependent circular dichroism (CD) and absorption spectra were then measured to follow duplex formation at 25°C (Figure 1c,d). Upon addition of (*S*,*S*)-**B** to a solution of template **1a** and 2 equiv of **A** that formed a 1:2 complex stabilized by amidinium-carboxylate salt bridges in $CDCl_3$, the absorption spectra changed slowly and reached equilibrium within 9 h, accompanied by a decrease in the first Cotton effect intensity in the long-wavelength region over 310 nm. Upon addition of (*R*,*R*)-**B**, the absorption spectra changed more rapidly, accompanied by a significant enhancement of Cotton effect intensities at 260−350 nm, reaching equilibrium within 3 h. These results suggest that duplex formation with (*R*,*R*)-**B** is much faster than with (*S*,*S*)-**B**. In addition, in both cases, the Cotton effect intensities after reaching equilibria were higher

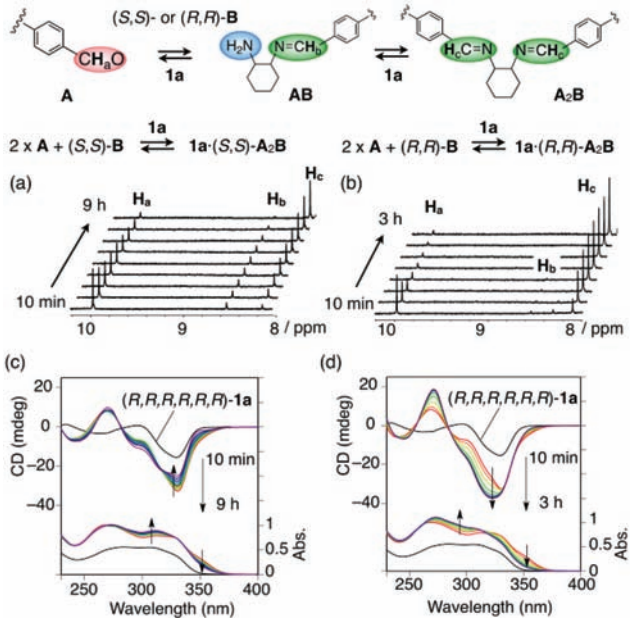

Figure 1. Time-dependent partial ^{1}H NMR (a,b) and CD and absorption (c,d) spectral changes of mixtures of 1.0 mM **A** and 0.5 mM (*S*,*S*)-**B** (a,c) or (*R*,*R*)-**B** (b,d) in the presence of 0.50 mM **1a** in $CDCl_3$ at 25°C.

than that of amidine template **1a** in the absorption region of the *p*-phenyleneethynylene residues (~270−370 nm), indicating that the duplexes of **1a** with (*S*,*S*)-$\mathbf{A_2B}$ and (*R*,*R*)-$\mathbf{A_2B}$ most likely adopted double-helical structure with a helix sense bias induced by chiral template **1a**, although their helical sense excesses might be different judging from their CD intensities because of the difference in the linker structures **B** with opposite configuration, resulting in the formation of a more preferred-handed double helix for the $\mathbf{1a{\cdot}}$(*R*,*R*)-$\mathbf{A_2B}$.

Imine-bond formation between **A** and racemic **B** was then investigated in the presence of **1a** in $CDCl_3$ at 25°C, because one of the enantiomers **B** was anticipated to react with **A** faster than the other, as predicted by the results in Figure 1, to form a preferred-handed complementary duplex with **1a**. Upon mixing of equimolar amounts of **A** and racemic **B** (1.0 mM each) in the presence of 0.5 mM **1a**, the aldehyde proton (H_a) intensity of **A** rapidly decreased, while two new imino proton peaks appeared (H_c(*S*,*S*) and H_c(*R*,*R*)), assigned to dimers (*S*,*S*)-$\mathbf{A_2B}$ and (*R*,*R*)-$\mathbf{A_2B}$, respectively (Figure S3a). The changes in the integral ratio of peaks H_c(*S*,*S*) and H_c(*R*,*R*) with time revealed that (*R*,*R*)-**B** reacted diastereoselectively with **A** over (*S*,*S*)-**B** to form duplex $\mathbf{1a{\cdot}A_2B}$ with diastereomeric excess (*de*) of 57% during the initial stage (15% conversion of **B**) under predominantly kinetic control assisted by chiral template **1a**. As the reaction progressed, the *de* gradually decreased as anticipated, reaching a constant value (30%) after ~3 h under totally thermodynamic control (run 1 in Table 1 and Figure S3b). We note that the *de* will vary significantly as a function of the conversion of **B**: lower conversion will lead to higher *de*. We attempted to measure the NMR spectrum of the mixture at lower conversion of **B**, but it was difficult because of the long acquisition time (10 min). Therefore, we calculated the selectivity factor (*s*) for qualitative comparison of the diastereoselectivity of the amidine template (Table 1) assuming that the present imine-bond formation could be regarded as a kind of kinetic resolution, at least initially. The changes in the

dx.doi.org/10.1021/ja301430h | *J. Am. Chem. Soc.* 2012, 134, 7250−7253

Table 1. Results of Diastereoselective Imine-Bond-Formations between A and Racemic B in the Presence of Chiral Amidine Templates 1−3

run	template	initial			at equilibrium			
		conv. of **B**[a] (%)	*de*[a] (%)	*s*[b]	time (h)	conv. of **B**[a] (%)	$\Delta\varepsilon_{1st}/\lambda$[c]	*de*[a] (%)
1	(*R*,*R*,*R*,*R*,*R*,*R*)-**1a**	15	57 (*R*,*R*)	4.0	3	48	−205/323	30 (*R*,*R*)
2	(*R*,*R*,*S*,*S*,*R*,*R*)-**1b**	13	32 (*R*,*R*)	2.0	4	49	−136/307	15 (*S*,*S*)
3	(*R*,*R*,*R*,*R*,*R*,*R*)-**1c**	27	0	1.0	1	50	−165/323	0
4	(*R*,*R*,*S*,*S*,*R*,*R*)-**1d**	14	4 (*R*,*R*)	1.1	2	50	−87/323	30 (*S*,*S*)
5	(*R*,*R*,*R*,*R*,*R*,*R*)-**1e**	4	52 (*R*,*R*)	3.2	2	43	−170/323	22 (*R*,*R*)
6	(*R*,*R*,*R*,*R*,*R*,*R*)-**1f**	19	0	1.0	12	43	−118/320	0
7	(*R*,*R*,*R*,*R*,*R*)-**1g**	1	0	1.0	12	35	−208/341	0
8	(*R*,*R*,*R*,*R*)-**1h**	3	58 (*R*,*R*)	3.8	12	15	−51/318	30 (*R*,*R*)
9	(*R*,*R*)-**2a**	9	8 (*R*,*R*)	1.2	2	50	−67/332	8 (*R*,*R*)
10	(*R*,*R*)-**2b**	6	0	1.0	3	44	7/322	0
11	(*R*,*R*)-**3a**	12	9 (*R*,*R*)	1.2	2	50	−82/332	9 (*R*,*R*)

[a]Estimated by ^{1}H NMR. [b]Selectivity factor determined using $s = k_{rel(fast/slow)} = \ln[1 - C(1 + de)]/\ln[1 - C(1 - de)]$, where C is the conversion of **B** and taking the *de* of $\mathbf{A_2B}$. [c]Units are $cm^{-1}M^{-1}/nm$.

patterns and intensities of the CD and absorption spectra of the mixture with time (Figure S3c) were similar to those observed for the mixture of **A** and (*R*,*R*)-**B**, which also supported preferential reaction of (*R*,*R*)-**B** over (*S*,*S*)-**B**, leading to a double helix of **1a**·(*R*,*R*)-$\mathbf{A_2B}$ with an excess helical sense.

Imine-bond formations between **A** and racemic **B** in the presence of templates consisting of optically pure (*R*,*R*)-amidine **1** and achiral amidines **2** and **3** linked through chiral (**L1**−**L5**) and achiral (**L6**) linkers were then investigated (Figures S4−S13) to gain insight into the effects of the amidine and linker chiralities and the stereostructures of the linkers on the diastereoselective imine-bond formations (Chart 1). These results are summarized in Table 1.

Template **1b**, in which the linker of **1a** was replaced by the corresponding (*S*,*S*)-enantiomer, also assisted (*R*,*R*)-selective imine-bond formation of **B** (32% *de*) during the initial stage. However, as the reaction proceeded, the selectivity reversed, and the opposite (*S*,*S*)-**B** was preferentially inserted after aldehyde **A** to form optically active duplex **1b**·$\mathbf{A_2B}$ (15% *de*) (run 2 and Figure S4), although the diastereoselectivity and hence the *s* value were lower than with **1a**, and the CD intensities during the reaction were weaker than for **1a**·$\mathbf{A_2B}$ duplexes. Thus the amidine chirality of the template appears to kinetically control the (*S*,*S*/*R*,*R*) selectivity of diamine **B** initially, but at equilibrium the selectivity is governed by the linker chirality under thermodynamic control, while the diastereoselectivity (*de* and *s*) may be determined by both the amidine and linker chiralities (see below).

Templates **1c**,**d**, with structural characteristics similar to those of **1a**,**b** except for the linker amide sequences, were used; amidine dimers **1c**,**d** are linked respectively by the (*R*,*R*)- or (*S*,*S*)-*trans*-cyclohexanedicarboxylic acid through an amide bond (**L2**). Surprisingly, template **1c** showed no diastereoselectivity toward racemic **B** during duplex formation of **1c**·$\mathbf{A_2B}$ (run 3 and Figure S5), whereas template **1d** displayed behavior similar to that of **1b**: (*R*,*R*)-**B** selectively reacted with **A** initially, but (*S*,*S*)-**B** was preferentially inserted at equilibrium, affording the **1d**·$\mathbf{A_2B}$ duplex (30% *de* of $\mathbf{A_2B}$) (run 4 and Figure S6), suggesting that the slight difference in the linker amide sequences of the templates significantly affects diastereoselectivity during imine-bond formation. Again, the linker stereochemistry ((*S*,*S*)-**L2**) determined the (*S*,*S*/*R*,*R*) selectivity of **B**.[16] The first Cotton intensities of these duplexes at equilibrium were almost proportional to the *de* values of $\mathbf{A_2B}$ produced at equilibrium (Figure S15), suggesting that the helical sense excess of the resulting duplex likely determines the diastereoselectivity of racemic **B** at equilibrium.

The *N*-methylated amide-linked (**L3**) chiral amidine dimer of **1a**, **1e**, showed good (*R*,*R*)-selectivity (52% *de*, *s* = 3.2 initially; 22% *de* at equilibrium) and slightly weaker Cotton effects compared to **1a** (run 5 and Figure S7). In contrast, template **1f**, having a flexible *N*-methylene linker (**L4**), exhibited no diastereoselectivity (run 6 and Figure S8), indicating that the amide bond (−NH−CO−) is not essential but the rigidity of the template backbones may be required for diastereoselective imine-bond formation. We then synthesized **1g**, a more rigid and bulkier template linked by the (*R*)-1,1′-binaphthyl-2,2′-diamine through an amide linkage (**L5**), which unexpectedly showed no diastereoselectivity (run 7 and Figure S9), probably due to the steric hindrance of the linker residue, and the duplex showed almost no change in its CD spectra before and after imine-bond formation.

Interestingly, **1h**, in which the linker of **1a** was replaced by an achiral rigid azobenzene unit (**L6**), also served as a good template, showing (*R*,*R*)-**B** selectivity of *s* = 3.8 during the initial stage despite its achiral linker (run 8 and Figure S10). This unexpectedly high diastereoselectivity suggests that chiral linkers may not be indispensable for the present diastereoselective imine-bond formation. We note, however, that template **1h** assisted the imine-bond formation in a rather low conversion at equilibrium (15%), probably because its azobenzene unit is too short to form a stable duplex with the resulting complementary $\mathbf{A_2B}$ strand; therefore, the reaction mixture containing a small amount of duplex showed almost no change in its CD spectra despite the high (*R*,*R*)-**B** selectivity.

The effect of amidine chirality on the diastereoselective imine-bond formation was then investigated in the presence of templates bearing achiral isopropyl (**2**) and cyclohexyl (**3**) amidines linked by the optically active rigid **L1** (**2a**, **3a**) and flexible **L4** (**2b**) linkers. As shown in Table 1 (runs 9−11 and Figures S11−S13), diastereoselectivities with **2a** and **3a** were poor (8 and 9% *de*, respectively), independent of the conversion, and **2b** showed no diastereoselectivity, as anticipated because of its flexible linker. However, templates **2a** and **3a** produced the (*R*,*R*)-rich dimers of **A**, revealing that the linker chirality contributes to determining the (*S*,*S*/*R*,*R*) selectivity of diamine **B**, although the diastereoselectivity is not high when the amidines are achiral.

Using template **2b**, the (*R*,*R*)-trans/(*R*,*S*)-cis selectivity of **B** was also examined. The product ratio of the (*R*,*R*)-$\mathbf{A_2B}$/(*R*,*S*)-$\mathbf{A_2B}$ dimers was estimated to be 76/24 (mol/mol) from ^{1}H NMR (Figure S14), indicating that **2b** can discriminate the diastereomers of *trans*- and *cis*-**B**, and *trans*-**B** was selectively inserted after monomer **A** during the template-assisted duplex formation.

From these results, we conclude that the chiral (*R*)-1-phenylethyl groups on the amidine residues mainly contribute to diastereoselective imine-bond formation during the initial stage under kinetic control, while the chirality of the *trans*-cyclohexane-based linkers determines the (*S*,*S*/*R*,*R*) selectivity and diastereoselectivity under thermodynamic control. Thus, the appropriate combination of rigid linkers with a specific handedness and chiral amidines appears to be important for achieving high diastereoselectivity during template-assisted imine-bond formation.

dx.doi.org/10.1021/ja301430h | *J. Am. Chem. Soc.* 2012, 134, 7250−7253

Table 2. Rate Constants ($M^{-1}s^{-1}$) of the Imine-Bond Formation between A and B in the Presence of 1a

$2\,\mathbf{A} + \mathbf{B} \underset{k_{-1}}{\overset{k_1}{\rightleftharpoons}} \mathbf{A} + \mathbf{AB} + H_2O \underset{k_{-2}}{\overset{k_2}{\rightleftharpoons}} \mathbf{A_2B} + 2\,H_2O$

diamine	k_1 [$M^{-1}s^{-1}$]	k_{-1} [$M^{-1}s^{-1}$]	k_2 [$M^{-1}s^{-1}$]	k_{-2} [$M^{-1}s^{-1}$]
(*R*,*R*)-**B**	1.4	0.23	8.1	9.0×10^{-4}
(*S*,*S*)-**B**	0.65	0.60	1.0	1.2×10^{-4}

Finally, to gain information about the rate constants of (*S*,*S*)- and (*R*,*R*)-**B** with **A** during two-step imine-bond formations along **1a**, the time-dependent ^{1}H NMR spectral changes (Figure 1a,b) were analyzed, and the concentrations of carboxylic acid monomer **A**, monoimine intermediate **AB**, and carboxylic acid dimer $\mathbf{A_2B}$ were plotted versus reaction time (Figure S1c,d), revealing that the imine-bond formations of (*R*,*R*)-**B** in each step assisted by **1a** reached equilibrium much faster than for (*S*,*S*)-**B**. It was difficult to estimate the rate constant at each step analytically due to the complicated two-step reversible reactions (Table 2). Thus, the kinetic data were fitted by numerical integration using the fourth-order Runge–Kutta method to estimate the rate constants (SI and Table 2). The rate constants for the first forward reaction (k_1) in the presence of **1a** at 25°C were estimated to be 1.4 $M^{-1}s^{-1}$ for (*R*,*R*)-**B** and 0.65 $M^{-1}s^{-1}$ for (*S*,*S*)-**B**, indicating that (*R*,*R*)-**B** reacted with **A** almost 2.2 times faster than (*S*,*S*)-**B** to form monoimine intermediate **AB**. During further reaction of **AB** with **A**, (*R*,*R*)-**AB** was found to react 8.1 times faster than (*S*,*S*)-**AB**, forming carboxylic acid dimer $\mathbf{A_2B}$ rich in (*R*,*R*)-**B**; the rate constants for the second forward reaction (k_2) along **1a** at 25°C were 8.1 $M^{-1}s^{-1}$ for (*R*,*R*)-**B** and 1.0 $M^{-1}s^{-1}$ for (*S*,*S*)-**B**.

This remarkable enhancement of the rate constants for **AB**, particularly (*R*,*R*)-**AB** in the second imine-bond formation, could be ascribed to ternary complexation of **1a**·**A**·(*R*,*R*)-**AB**, with the aldehyde group of **A** and the remaining amino group of (*R*,*R*)-**AB** much more favorably located than in **1a**·**A**·(*S*,*S*)-**AB** so as to form a complementary double helix with helix sense bias assisted by the chiral amidine of **1a**. Therefore, in the second imine-bond formation, the (*S*,*S*/*R*,*R*) selectivity and its diastereoselectivity of racemic **B** could be mainly controlled by the amidine chirality of the chiral amidine templates initially, but both the amidine and linker chiralities contribute at equilibrium.

We believe the present findings will contribute to developing more sophisticated template-assisted asymmetric replication using complementary chiral amidinium-carboxylate salt bridges.

■ ASSOCIATED CONTENT

Ⓢ Supporting Information

Experimental details. This material is available free of charge via the Internet at http://pubs.acs.org.

■ AUTHOR INFORMATION

Corresponding Author

yashima@apchem.nagoya-u.ac.jp

Notes

The authors declare no competing financial interest.

■ ACKNOWLEDGMENTS

Supported by Grant-in-Aids for Scientific Research (S) from JSPS (E.Y.), for Scientific Research on Innovative Areas, "Emergence in Chemistry" (20111010, Y.F.) from MEXT, and JSPS Research Fellowship for Young Scientists (2728, H.Y.).

■ REFERENCES

(1) (a) Polowinski, S. *Template Polymerization*; ChemTec Publishing: Ontario, 1997. (b) Diederich, F.; Stang, P. J. *Templated Organic Synthesis*; Wiley-VCH: Weinheim, 2000.

(2) Reviews on template-directed polymerization and template synthesis: (a) Inaki, Y.; Takemoto, K. *Adv. Polym. Sci.* **1981**, *41*, 1. (b) Hoss, R.; Vögtle, F. *Angew. Chem., Int. Ed. Engl.* **1994**, *33*, 375. (c) Tan, Y. Y. *Prog. Polym. Sci.* **1994**, *19*, 561. (d) Leitzel, J. C.; Lynn, D. G. *Chem. Rec.* **2000**, *1*, 53. (e) Summerer, D.; Marx, A. *Angew. Chem., Int. Ed.* **2002**, *41*, 89. (f) Polowinski, S. *Prog. Polym. Sci.* **2002**, *27*, 537. (g) Li, X.; Liu, D. R. *Angew. Chem., Int. Ed.* **2004**, *43*, 4848. (h) Silverman, A. P.; Kool, E. T. *Chem. Rev.* **2006**, *106*, 3775. (i) Svoboda, J.; König, B. *Chem. Rev.* **2006**, *106*, 5413. (j) Prins, L. J.; Scrimin, P. *Angew. Chem., Int. Ed.* **2009**, *48*, 2288.

(3) Böhler, C.; Nielsen, P. E.; Orgel, L. E. *Nature* **1995**, *376*, 578. Ura, Y.; Beierle, J. M.; Leman, L. J.; Orgel, L. E.; Ghadiri, M. R. *Science* **2009**, *325*, 73.

(4) Goodwin, J. T.; Lynn, D. G. *J. Am. Chem. Soc.* **1992**, *114*, 9197. Zhan, Z.-Y. J.; Lynn, D. G. *J. Am. Chem. Soc.* **1997**, *119*, 12420. Li, X.; Zhan, Z.-Y. J.; Knipe, R.; Lynn, D. G. *J. Am. Chem. Soc.* **2002**, *124*, 746.

(5) Li, X.; Liu, D. R. *J. Am. Chem. Soc.* **2003**, *125*, 10188.

(6) Rosenbaum, D. M.; Liu, D. R. *J. Am. Chem. Soc.* **2003**, *125*, 13924. Kleiner, R. E.; Brudno, Y.; Birnbaum, M. E.; Liu, D. R. *J. Am. Chem. Soc.* **2008**, *130*, 4646.

(7) Lee, D. H.; Granja, J. R.; Martinez, J. A.; Severin, K.; Ghadiri, M. R. *Nature* **1996**, *382*, 525. Yao, S.; Ghosh, I.; Zutshi, R.; Chmielewski, J. *J. Am. Chem. Soc.* **1997**, *119*, 10559. Krishnan-Ghosh, Y.; Balasubramanian, S. *Angew. Chem., Int. Ed.* **2003**, *42*, 2171.

(8) Kelly, T. R.; Zhao, C.; Bridger, G. J. *J. Am. Chem. Soc.* **1989**, *111*, 3744. Tjivikua, T.; Ballester, P.; Rebek, J., Jr. *J. Am. Chem. Soc.* **1990**, *112*, 1249. Terfort, A.; von Kiedrowski, G. *Angew. Chem., Int. Ed. Engl.* **1992**, *31*, 654. Wang, B.; Sutherland, I. O. *Chem. Commun.* **1997**, 1495. Kassianidis, E.; Philp, D. *Angew. Chem., Int. Ed.* **2006**, *45*, 6344.

(9) Serizawa, T.; Hamada, K.-i.; Akashi, M. *Nature* **2004**, *429*, 52. Lin, N.-T.; Lin, S.-Y.; Lee, S.-L.; Chen, C.-h.; Hsu, C.-H.; Hwang, L. P.; Xie, Z.-Y.; Chen, C.-H.; Huang, S.-L.; Luh, T.-Y. *Angew. Chem., Int. Ed.* **2007**, *46*, 4481. Lo, P. K.; Sleiman, H. F. *J. Am. Chem. Soc.* **2009**, *131*, 4182.

(10) Roelfes, G. *Mol. Biosyst.* **2007**, *3*, 126.

(11) Recent reviews on synthetic double helices: Hecht, S.; Huc, I. *Foldamers: Structure, Properties, and Applications*; Wiley-VCH: Weinheim, 2007. Furusho, Y.; Yashima, E. *Chem. Rec.* **2007**, *7*, 1. Amemiya, R.; Yamaguchi, M. *Org. Biomol. Chem.* **2008**, *6*, 26. Saraogi, I.; Hamilton, A. D. *Chem. Soc. Rev.* **2009**, *38*, 1726. Haldar, D.; Schmuck, C. *Chem. Soc. Rev.* **2009**, *38*, 363. Juwarker, H.; Jeong, K.-S. *Chem. Soc. Rev.* **2010**, *39*, 3664. Guichard, G.; Huc, I. *Chem. Commun.* **2011**, *47*, 5933.

(12) Artificial double helices based on amidinium-carboxylate salt bridges: Tanaka, Y.; Katagiri, H.; Furusho, Y.; Yashima, E. *Angew. Chem., Int. Ed.* **2005**, *44*, 3867. Hasegawa, T.; Furusho, Y.; Katagiri, H.; Yashima, E. *Angew. Chem., Int. Ed.* **2007**, *46*, 5885. Ito, H.; Furusho, Y.; Hasegawa, T.; Yashima, E. *J. Am. Chem. Soc.* **2008**, *130*, 14008. Ito, H.; Ikeda, M.; Hasegawa, T.; Furusho, Y.; Yashima, E. *J. Am. Chem. Soc.* **2011**, *131*, 3419.

(13) Yamada, H.; Furusho, Y.; Ito, H.; Yashima, E. *Chem. Commun.* **2010**, *46*, 3487.

(14) Recent examples: Oh, K.; Jeong, K. S.; Moore, J. S. *Nature* **2001**, *414*, 889. Chichak, K. S.; Cantrill, S. J.; Pease, A. R.; Chiu, S.-H.; Cave, G. W. V.; Atwood, J. L.; Stoddart, J. F. *Science* **2004**, *304*, 1308. Campbell, V. E.; Hatten, X.; Delsuc, N.; Kauffmann, B.; Huc, I.; Nitschke, J. R. *Nat. Chem.* **2010**, *2*, 684. Belowich, M. E.; Stoddart, J. F. *Chem. Soc. Rev.* **2012**, *41*, 2003.

(15) In the absence of the template, carboxylic acid monomer **A** self-catalyzed the reaction with **B**, giving complexed mixtures of monomer (**AB**) and dimer ($\mathbf{A_2B}$) (Figure S16).

(16) Similar amide-sequence effect: Goto, K.; Moore, J. S. *Org. Lett.* **2005**, *7*, 1683.